©2020 IEEE. Personal use of this material is permitted. Permission from IEEE must be obtained for all other uses, in any current or future media, including reprinting/republishing this material for advertising or promotional purposes, creating new collective works, for resale or redistribution to servers or lists, or reuse of any copyrighted component of this work in other works.

Digital Object Identifier 10.1109/ECCE44975.2020.9236020

2020 IEEE Energy Conversion Congress and Exposition (ECCE)

Scalable State-Space Model of Voltage Source Converter for Low-Frequency Stability Analysis

Federico Cecati

Rongwu Zhu

Marius Langwasser

Marco Liserre

Xiongfei Wang

Suggested Citation

F. Cecati, R. Zhu, M. Langwasser, M. Liserre and X. Wang, "Scalable State-Space Model of Voltage Source Converter for Low-Frequency Stability Analysis," 2020 IEEE Energy Conversion Congress and Exposition (ECCE), Detroit, MI, USA, 2020.

Scalable State-Space Model of Voltage Source Converter for Low-Frequency Stability Analysis

Federico Cecati*, Rongwu Zhu*, Marius Langwasser* Marco Liserre*, Xiongfei Wang†
*Chair of Power Electronics, *Christian-Albrechts-Universität* Kiel, Germany
†Department of Energy Technology, *Aalborg University*, Aalborg, Denmark
fc@tf.uni-kiel.de, rzh@tf.uni-kiel.de, mlan@tf.uni-kiel.de, ml@tf.uni-kiel.de, xwa@et.aau.dk

***Abstract*—Low frequency instability phenomena in power electronic based power systems can originate both at converter and at power system level. At the converter level, the interaction between PLL, dc-link and ac voltage control in voltage source converters (VSCs) connected to a weak grid can lead to instability. At the power system level, the interactions among different parallel VSCs can produce oscillatory phenomena, and even result in instability. However, a model to study the instability phenomena at both levels is still under development. In this paper, a scalable VSC state space model, which captures the interactions among PLL, dc-link and ac voltage control is proposed. The proposed model is suitable for interconnection, and an example of power system modeling is shown. The model is then validated through simulations and experimental tests. Eigenvalue analysis is carried out to investigate the influence of the control parameters on the stability.**

***Index Terms*—Low Frequency Stability, Voltage Source Converter, Scalable State-Space Model**

I. Introduction

Voltage source converters (VSCs) have become nowadays very common in modern power systems [1]–[4]. Nevertheless, in weak grid conditions, the interaction between PLL, dc-link voltage and ac voltage control can cause instability phenomena at converter level [1]. Several studies analyze the instability phenomena due to the PLL [5]–[7], the dc-link voltage control [1], [8], and the ac voltage control [2], [9]. However, there are still few studies which realize a complete model and analyze all the three control loops together.

The system level stability analysis needs a state-space model of the power grid. This can be realized when the ac voltage at each node of the grid is an output variable of the VSC, and all these voltages are expressed in a common DQ reference frame. This feature is referred to as scalability of the VSC model. The model in [1] does not present the converter output voltage neither as a state nor input/output variable, thus does not have the scalability. In [10] the phenomena of parallel VSC interactions is dealt, but no state-space model of the power system is provided. The models in [2] and [9] are suitable for interconnection, since the VSC output voltage is a state variable inherited from the filter capacitor. However, the modelling of the LCL filter increases the system order and introduces high frequency resonances out of the study object. Moreover, L-filtered power converters, including multilevel converters which are becoming very common in the power grid, can not be modelled with this approach. Furthermore, in [2], the dc-link voltage dynamics is not considered. The great challenge for the dc-link voltage dynamic modelling is its strong nonlinearity, which can not be handled with the linearisation method used in [2].

In this paper, a scalable state-space model of a VSC is derived. The model presents the following features and novelties:

- It includes all the outer loops dynamics, whose interactions originate unstable dynamics: PLL, dc-link and ac voltage control.
- It has the ac voltage as output variable and is suitable for multi-VSC power systems modeling and analysis (scalability feature).
- The VSC model is nonlinear: a nonlinear interconnection procedure is proposed to build up nonlinear power system model. That allows to easily compute the equilibrium point of the whole grid, useful for the linearization.
- The VSC model does not include the filter, thus is suitable also for L-filtered converters, including multilevel converters.

The paper is structured as follows: in Section 2, a description of the system under consideration is reported and the inner loop modeling is addressed, Section 3 presents the state-space model of the whole VSC and shows and example of interconnection, and in Section 4 the derived model is used for an eigenvalue analysis and validated through time domain simulations and experimental results.

The authors gratefully acknowledge funding by German Federal Ministry for Economic Affairs and Energy within the research project "Add-On" (0350022B) and by Gesellschaft für Energie und Klimaschutz Schleswig-Holstein GmbH (EKSH) doctoral studies grant.

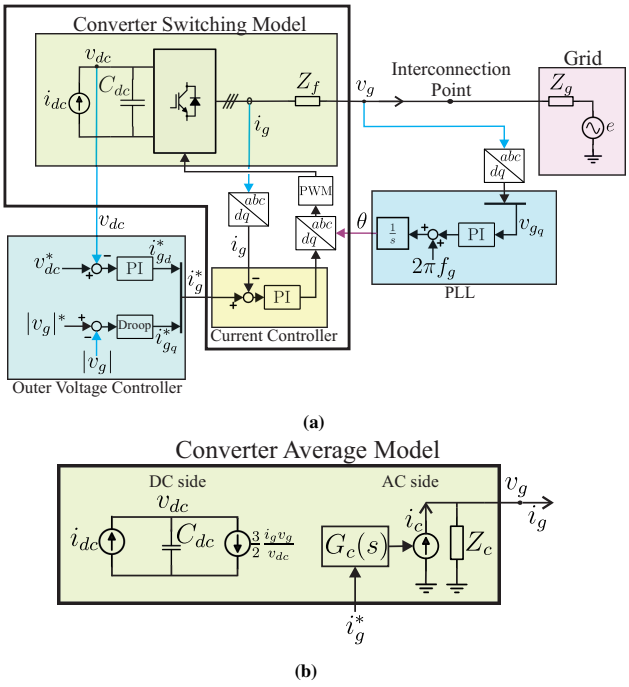

Figure 1: A three-phase grid-connected VSC implementing output voltage controller, inner current controller and SFR-PLL. (a) Complete switching model (b) Average model of the inverter.

II. System Description and Inner Loop Modeling

The principle scheme of the considered grid connected VSC is depicted in Fig. 1(a). The current source i_{dc} models the upstream primary energy source, i.e. the photovoltaic module or the wind turbine. The current inner loop is implemented by means of a PI regulator. The dc-link voltage is controlled with a PI controller, the ac voltage with droop controller and a synchronous reference frame Phase Locked Loop (SRF-PLL) is implemented for the synchronization. The converter is connected to the grid with an impedance Z_g composed of a resistor R_g in series with a inductor L_g. The VSC presents a L filter represented with an impedance Z_f including the inductor filter L_f and the parasitic resistance R_f. In low frequency range, LCL filter can be approximated with a L filter neglecting the capacitor, thus the proposed model can be used also for LCL filtered converters.

A. Modeling of the ac side and the inner current loop

The ac side of the converter is often modeled in several state-space models in literature with an ideal voltage source, representing the inverter, in series with the filter inductor L_f [2], [8], [9], [11], [12]. With this modeling strategy, no parallel impedance is present in the converter output, thus the VSC output voltage can not be obtained as variable. The paper [2] highlighted as this feature represents a limitation for the modeling of multi-VSC power systems, and proposed to introduce a virtual resistor at each node of the grid. Nevertheless, this solution can lead to inaccurate results and numerical problems [13].

In this paper, a VSC state-space model is proposed in order to overcome the above-mentioned challenge. The proposed solution is to model the converter and the inner current loop using impedance-based modeling, as shown in Fig. 1(b). In this way, the parallel impedance Z_c, representing the inner current loop, is obtained and can be exploited to get the output voltage v_g as variable. The obtained impedance model of the inner loop is then converted in state-space form, and merged with the model of the outer loops and the dc-link dynamics.

Considering the standard PI current controller with decoupling terms [3], expressing voltages and currents as complex variables, e.g. $i_g = i_{g_d} + j i_{g_q}$, the equation of the inner loop can be written as:

$$v_c = (i_g^* - i_g)\left(K_p + \frac{K_i}{s}\right) + j\omega L_f i_g \tag{1}$$

$$i_g = \frac{v_c - v_g}{L_f(s + j\omega)} \tag{2}$$

By substituting (1) into (2), the current i_g can be expressed as:

$$i_g = G_c(s) i_g^* - Y_c(s) v_g \tag{3}$$

being $Y_c(s) = \frac{1}{Z_c}$, and the transfer functions $G_c(s)$ and $Y_c(s)$:

$$\begin{cases} G_c(s) = \dfrac{K_p s + K_i}{L_f s^2 + K_p s + K_i} \\ Y_c(s) = \dfrac{s}{L_f s^2 + K_p s + K_i} \end{cases} \tag{4}$$

In (4), $G_c(s)$ and $Y_c(s)$ posses the same denominator with two poles in:

$$p_{1,2} = \frac{-K_p \mp \sqrt{K_p^2 - 4K_i L_f}}{2L_f} \tag{5}$$

Regarding the pole p_1, assuming technical optimum tuning, i.e. $K_i = \frac{K_p R_f}{L_f}$, (5) can be rewritten as

$$p_1 = \frac{-K_p - \sqrt{K_p^2 - 4K_p R_f}}{2L_f} \tag{6}$$

Assuming $K_p \gg 4R_f$, the term $4K_p R_f$ is neglected, and (6) becomes

$$\frac{-K_p - \sqrt{K_p^2}}{2L_f} = -\frac{K_p}{L_f} \tag{7}$$

Regarding the pole p_2, (5) can be rewritten as

$$p_2 = \frac{-K_p + K_p\sqrt{1 - 4\frac{K_i L_f}{K_p^2}}}{2L_f} \tag{8}$$

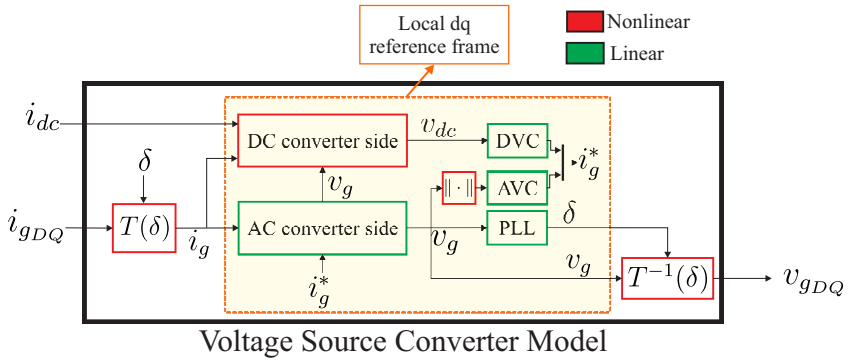

Figure 2: The graphical representation of the proposed VSC model in all its parts and their relations.

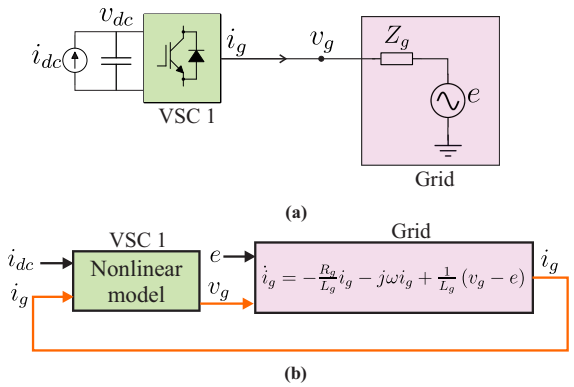

Figure 3: The interconnection of the proposed VSC with the grid. The arrows are highlighted in orange when represent interconnections between blocks.

considering the first order Taylor expansion $\sqrt{1+x} = 1 + \frac{1}{2}x + o(x)$, (8) becomes:

$$\frac{K_p\left(-1+1-2\frac{K_i L_f}{K_p^2}\right)}{2L_f} = \frac{-2\frac{K_i L_f}{K_p}}{2L_f} = -\frac{K_i}{K_p} \tag{9}$$

In the transfer $G_c(s)$, the pole in $\frac{K_i}{K_p}$ simplifies with the zero in $\frac{K_i}{K_p}$, and only the pole in $\frac{K_p}{L_f}$ remains. With this simplification, $G_c(s)$ becomes a lowpass filter with cutoff frequency equal to the bandwidth of the current loop, circa $\frac{K_p}{L_f}$ [3].

$$G_c(s) = \frac{1}{1 + \frac{L_f}{K_p}s} \tag{10}$$

Conversely, in $Y_c(s)$ the pole in $\frac{K_p}{L_f}$ is neglected, and only the pole in $\frac{K_i}{K_p}$ remains. This approximation is valid under the assumption that the disturbances from the grid under analysis has a bandwidth lower then $\frac{K_p}{L_f}$. Since this paper studies the low frequency dynamics of grid connected VSC, the assumption is valid. With these assumptions, the transfer functions in (4) becomes:

$$Y_c(s) = \frac{s}{K_p s + K_i} \tag{11}$$

Equation (3), expressed in Laplace domain, can be converted in state-space form considering (10) and (11). For that, vectorial notation for currents and voltages is employed, e.g. $i_g = \begin{pmatrix} i_{g_d} \\ i_{g_q} \end{pmatrix}$. The resulting state-space model of the inverter current loop is:

$$\begin{cases} \dot{v}_{cc} = K_i i_c - K_i i_g \\ \dot{i}_c = -\frac{K_p}{L} i_c + \frac{K_p}{L} i_g^* \\ v_g = K_p\left(i_c - i_g\right) + v_{cc} \end{cases} \tag{12}$$

where v_{cc} is the auxiliary state-space variable used to express v_g.

III. VSC Modeling and Interconnection

The obtained current loop model (12) is then merged with the rest of the VSC model. The dc-link voltage controller, ac voltage controller, and the PLL can be modeled with a similar procedure of [1], [2]. The dc-link dynamics is modeled with the power balance equation [3]. The interrelation of the converter hardware and control parts is graphically explained in Fig. 2. In order to make the proposed model feasible for a system level stability analysis the inputs and outputs must be expressed in a global DQ reference frame aligned with the grid voltage e, common for all the VSCs of the power grid [2]. The VSC control is realized in a local dq frame aligned with the VSC output voltage v_g, in order to decouple the active and reactive component of the current [3]. For this reason, a change of reference frame operated through a Park transformation matrix $T(\delta)$, as shown in Fig. 2, is necessary [2]. The variables expressed in the global DQ have a pedix, e.g. $i_{g_{DQ}}$, while the variables expressed in the local dq frame have no pedix, e.g. i_g.

From Fig. 2, it emerges the scalable structures of the model: the dc current i_{dc} and the grid current $i_{g_{DQ}}$ at the interconnection point are the inputs, and the ac

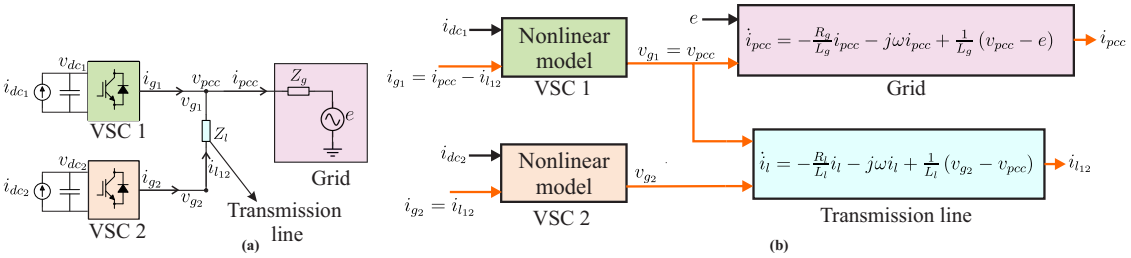

Figure 4: The proposed interconnection procedure in power system with two VSCs. (a) The power system scheme. (b) The model interconnection procedure.

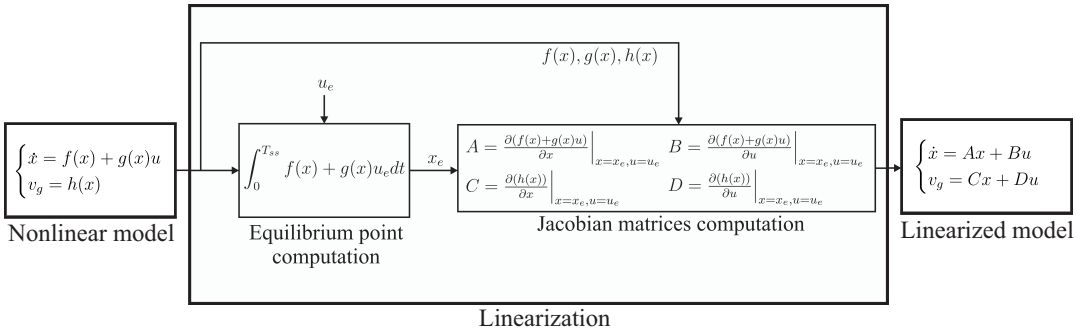

Figure 5: The proposed linearisation procedure around the operating point defined by (x_e, u_e).

voltage $v_{g_{DQ}}$ at the interconnection point is the output. The model has therefore the form:

$$\dot{x} = f(x) + g(x) \begin{pmatrix} i_{dc} \\ i_{g_{DQ}} \end{pmatrix} \tag{13}$$

$$v_{g_{DQ}} = h(x) \tag{14}$$

This structure allows the interconnection of the VSC both with other VSCs in parallel, and with the electric grid.

A. Single VSC model connected to the grid

The nonlinear state-space model of the VSC interconnected with the grid as in Fig. 3, in the local dq frame, has the form:

$$\begin{cases} \dot{i}_c = -\frac{K_p}{L} i_c + \frac{K_p}{L} i_g^* \\ \dot{v}_{dc} = -\frac{3}{2}\frac{1}{C_{dc}}\frac{v_g \cdot i_g}{v_{dc}} + \frac{1}{C_{dc}} i_{dc} \\ \dot{\Phi}_{dc} = v_{dc} - v_{dc}^* \\ \dot{\delta} = \begin{pmatrix} 0 & K_{p,PLL} \end{pmatrix} v_g + K_{i,PLL} \Phi_q \\ \dot{\Phi}_q = \begin{pmatrix} 0 & 1 \end{pmatrix} v_g \\ \dot{v_{cc}} = -K_i i_g + K_i i_c \\ \dot{i}_g = \frac{R_g}{L_g} i_g - \Omega i_g + \frac{1}{L_g} v_g - \frac{1}{L_g} T(\delta) e_{DQ} \end{cases} \tag{15}$$

$$\begin{cases} \Omega = \begin{pmatrix} 0 & -2\pi 50 \\ 2\pi 50 & 0 \end{pmatrix} \\ T(\delta) = \begin{pmatrix} \cos\delta & \sin\delta \\ -\sin\delta & \cos\delta \end{pmatrix} \\ v_g = K_p \left(i_c - i_g\right) + v_{cc} \\ i_g^* = \begin{pmatrix} K_{p,DC}(v_{dc} - v_{dc}^*) + K_{i,DC}\Phi_{dc} \\ K_{p,AC}(v_g^* - \sqrt{v_g \cdot v_g}) \end{pmatrix} \end{cases} \tag{16}$$

The state-space model of the grid, shown as a block in Fig. 3(b), has the grid voltage e and the voltage v_g as inputs, and PCC current i_g as output. The interconnection between VSC and grid is done through the variables v_g and i_g, connected as in Fig. 3(b). The resulting interconnected model (converter and grid), presents two inputs: the grid voltage e and the dc current of the converter i_{dc}.

B. Parallel connection of VSCs

An important novelty of the proposed model is its suitability for interconnection with other VSCs. In Fig. 4(a), an example of power system with 2 VSCs is depicted. The proposed interconnection procedure is graphically explained in Fig. 4(b). All the variables are expressed in the global DQ frame, but the pedix DQ is omitted for compactness of notation. A power grid with two connected VSCs is considered. The VSC 1 is directly connected to the point of common coupling (PCC), while the VSC 2 is connected through a transmission line represented with an impedance $Z_l = R_l + sL_l$. From the output voltages v_{g_1} and v_{g_2} of the VSC 1 and 2

respectively, the current flowing in the impedance Z_l, which models the transmission line, can be computed with the RL branch equation, shown in the transmission line block of Fig. 4. The current i_{pcc} flowing in the grid is computed with the same RL branch equation, shown in the grid block. The interconnection of the VSCs is realized through the voltage equality $v_{g_1} = v_{pcc}$ and the node equation $i_{g_1} = i_{pcc} - i_{l_{12}}$. The inputs of the overall model are the grid voltage e and the currents i_{dc_1} an i_{dc_2} which define the active power injected by the VSCs.

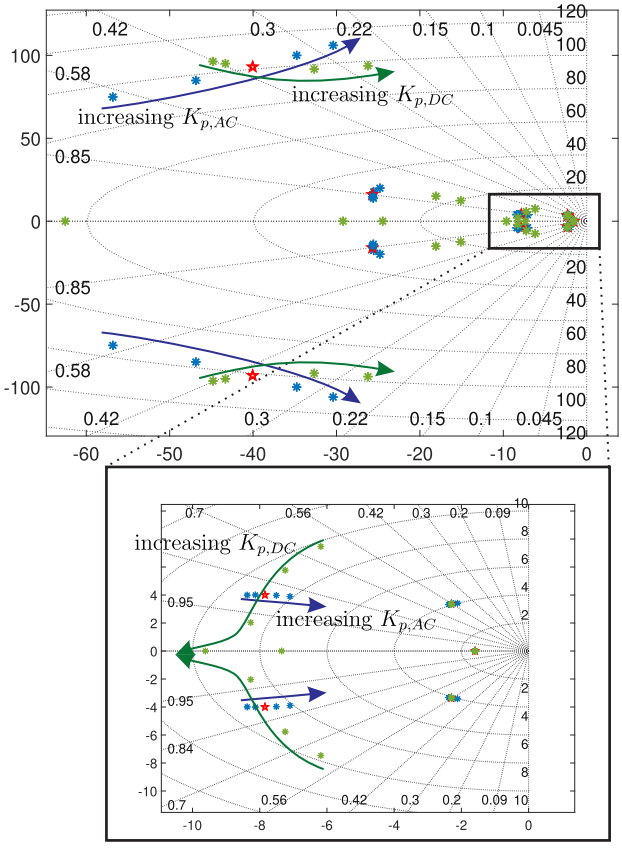

Figure 6: Eigenvalue analysis depending on the dc-link and ac voltage control parameters variations. The red star is the tuning used in the simulation.

IV. Eigenvalue Analysis

The proposed nonlinear model can be used for the power system stability analysis. Eigenvalue analysis is a very powerful tool which allows to identify frequency and damping ratio of all the dynamic modes of the grid [14] [15]. However, it needs a linear model of the power system, thus a linearisation of (15) is necessary. The small-signal linearisation procedure used in [2] is not suitable to linearise the equation of $\dot{v}_{dc}$ in (15). The Jacobian matrix computation, used in [9], is instead a valid approach for the nonlinear systems (15) [16], [17]. Nevertheless, the paper [9] as well as [1], [2], [8], [12],

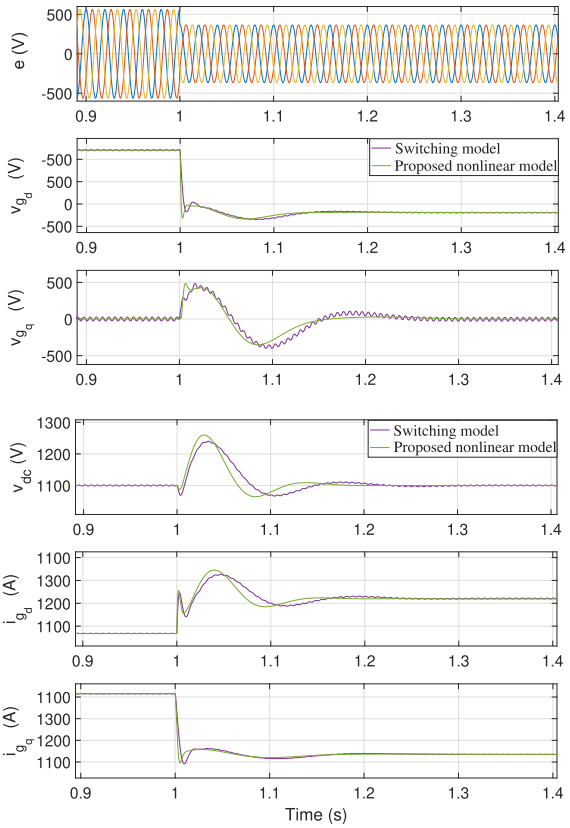

Figure 7: Proposed nonlinear model validation in simulation.

[18] do not focus on the computation of the linearisation equilibrium point, and its role in the eigenvalue analysis.

The procedure for the linearization used in this paper is explained in Fig. 5. The operating point is defined by the steady state input u_e, and the equilibrium point x_e is computed by integrating the nonlinear model. The obtained linearized model is used for the eigenvalue analysis.

In Fig. 6 the ac voltage proportional gain and the dc-link voltage controller bandwidth are varied in the range of 5-25 and 21.3-34 Hz respectively, and their influence on the stability is studied. In the high frequency, increasing $K_{p,DC}$ and $K_{p,AC}$ results in low damped modes. However, the eigenvalue shift is not the same in the two cases. By increasing $K_{p,DC}$, an increase in the natural frequency of the dynamic mode can be observed, beside the decrease in the damping. The increase of $K_{p,AC}$ results conversely in a modest decrease of the natural frequency. The situation is different in the low frequencies, which can be observed in the zoomed frame of Fig. 6. By increasing $K_{p,AC}$, a right shift of the eigenvalues can be noticed. Contrariwise, by increasing $K_{p,DC}$ a significant increase in the system damping can be observed in the low frequency.

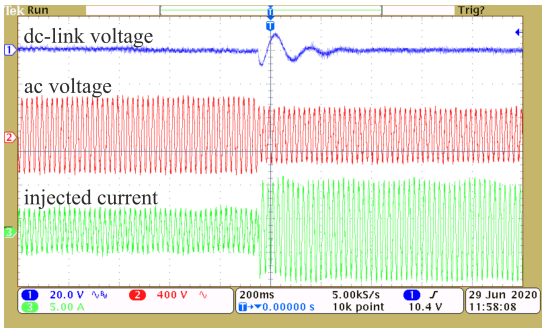

(a)

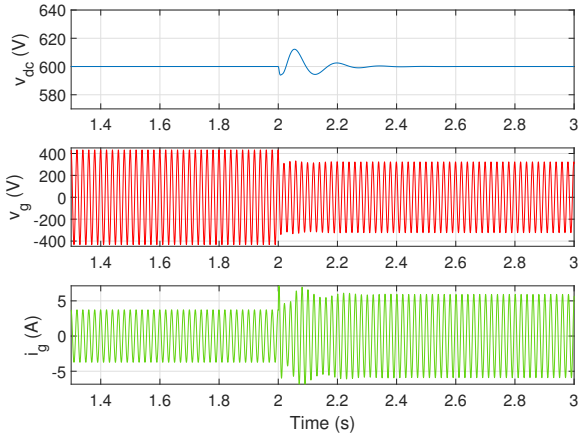

(b)

Figure 8: Proposed nonlinear model experimental validation.

V. Simulation and Experimental Validation

The proposed nonlinear model (15) is used to simulate a 2 MW VSC-based wind turbine connected to the grid. The considered grid has a SCR=3.5 and a R/X ratio equal to 0.1. A symmetrical voltage sag of 0.35 p.u. is simulated at $t = 1$, and the switching model behaviour is compared with the proposed nonlinear model, as shown in Fig. 7. Thereafter, a MicroLabBox-controlled 2 kW VSC is built up for the experimental model validation. The same simulation with a symmetrical voltage sag of 0.35 p.u. is performed and shown in Fig. 8. Both the simulation results and the experimental results highlight the high accuracy of the proposed nonlinear model respect to the real model.

VI. Conclusions

The proposed nonlinear VSC model presents a good accuracy respect to the detailed model in the low frequency range. The eigenvalue analyses depending on the dc-link voltage controller bandwidth and ac voltage control proportional gain have been realized and highlight the influence of these parameters on the stability. It has been shown that the outer control loops have a relevant influence in the VSC dynamics and are strongly coupled between them.

Moreover, the proposed model presents as output variable the VSC output voltage, expressed in a global DQ reference frame. This feature makes the VSC model suitable for interconnection with other VSCs and appropriate for the modeling and stability analysis of multi-VSC power systems. The interconnection capability is demonstrated by modeling a power system with two VSCs.

References

[1] Y. Huang *et al.*, "Modeling of vsc connected to weak grid for stability analysis of dc-link voltage control," *IEEE Journal of Em.and Sel. Topics in P.E.*, vol. 3, no. 4, pp. 1193–1204, 2015.

[2] N. Pogaku, M. Prodanovic, and T. C. Green, "Modeling, analysis and testing of autonomous operation of an inverter-based microgrid," *IEEE TPEL*, vol. 22, no. 2, pp. 613–625, 2007.

[3] R. Teodorescu, M. Liserre, and P. Rodriguez, *Grid converters for photovoltaic and wind power systems*. John Wiley & Sons, 2011, vol. 29.

[4] F. Blaabjerg, Y. Yang, D. Yang, and X. Wang, "Distributed power-generation systems and protection," vol. 105, no. 7, pp. 1311–1331, 2017.

[5] C. Zhang, X. Wang, and F. Blaabjerg, "Analysis of phase-locked loop influence on the stability of single-phase grid-connected inverter," in *2015 IEEE 6th International Symposium on Power Electronics for Distributed Generation Systems (PEDG)*. IEEE, 2015, pp. 1–8.

[6] D. Dong, B. Wen, D. Boroyevich, P. Mattavelli, and Y. Xue, "Analysis of phase-locked loop low-frequency stability in three-phase grid-connected power converters considering impedance interactions," vol. 62, no. 1, pp. 310–321, Jan 2015.

[7] X. Zhang, D. Xia, Z. Fu, G. Wang, and D. Xu, "An improved feedforward control method considering pll dynamics to improve weak grid stability of grid-connected inverters," vol. 54, no. 5, pp. 5143–5151, Sep. 2018.

[8] N. Bottrell, M. Prodanovic, and T. C. Green, "Dynamic stability of a microgrid with an active load," vol. 28, no. 11, pp. 5107–5119, Nov 2013.

[9] M. Rasheduzzaman *et al.*, "Reduced-order small-signal model of microgrid systems," *IEEE Trans on Sust. En.*, vol. 6, no. 4, pp. 1292–1305, Oct 2015.

[10] Y. Huang *et al.*, "Modeling and stability analysis of dc-link voltage control in multi-vscs with integrated to weak grid," *IEEE Trans. on En. Conv.*, vol. 32, no. 3, pp. 1127–1138, Sep. 2017.

[11] M. Rasheduzzaman, J. A. Mueller, and J. W. Kimball, "An accurate small-signal model of inverter- dominated islanded microgrids using *dq* reference frame," *IEEE Journal of Emerging and Selected Topics in Power Electronics*, vol. 2, no. 4, pp. 1070–1080, Dec 2014.

[12] F. Cecati, M. Andresen, R. Zhu, Z. Zou, and M. Liserre, "Robustness analysis of voltage control strategies of smart transformer," in *IECON 2018 - 44th Annual Conference of the IEEE Industrial Electronics Society*, Oct 2018, pp. 5566–5573.

[13] F. B. Hildebrand, *Introduction to numerical analysis*. Courier Corporation, 1987.

[14] P. Kundur, N. J. Balu, and M. G. Lauby, *Power system stability and control*. McGraw-hill New York, 1994, vol. 7.

[15] G. F. Franklin, J. D. Powell, A. Emami-Naeini, and J. D. Powell, *Feedback control of dynamic systems*. Addison-Wesley Reading, MA, 1994, vol. 3.

[16] H. K. Khalil and J. W. Grizzle, *Nonlinear systems*. Prentice hall Upper Saddle River, NJ, 2002, vol. 3.

[17] A. Isidori, "Nonlinear control systems springer-verlag," 1989.

[18] Y. Wang, X. Wang, Z. Chen, and F. Blaabjerg, "Small-signal stability analysis of inverter-fed power systems using component connection method," *IEEE Transactions on Smart Grid*, vol. 9, no. 5, pp. 5301–5310, Sep. 2018.